Unified Constant-frequency Integration Control of Three-phase Standard Bridge Boost Rectifier

Chongming Qiao and Keyue M. Smedley
Department of Electrical and Computer Engineering
University of California, Irvine, CA 92697
Tel: (949) 824-6710, Fax: (949) 824-3203, email: smedley@ uci.edu

Abstract: In this paper, a three-phase six-switch standard boost rectifier with unity-power-factor-correction is investigated. A general equation is derived that relates input phase voltage and duty ratios of switches in continuous conduction mode. Based on one of solutions and using One-Cycle Control, a Unified Constant-frequency Integration (UCI) controller for power-factor-correction (PFC) is proposed. For the standard bridge boost rectifier, unity-power-factor and low total-harmonic-distortion (THD) can be realized in all three phases with a simple circuit that is composed of one integrator with reset along with several flips-flops, comparators, and some logic and linear components. It does not require multipliers and three-phase voltage sensors, which are used in many other control approaches. In addition, it employs constant switching frequency modulation that is desirable for industrial applications. The proposed control approach is simple and reliable. Theoretical analysis is verified by simulation and experimental results.

1 Introduction.

Traditional diode rectifiers and thyristor rectifiers draw pulsed current from the ac main, causing significant current harmonics pollution. The international standards presented in IEC 1000-3-2 and EN61000-3-2 imposed harmonic restrictions to modern rectifiers, which results in a focused research effort on the topic of unity power factor rectifiers. Three-phase PFC rectifiers are preferred for high power applications due to their symmetric current drawing characteristics. Many topologies have been proposed recently [1]-[4]. Among them, the six-switch bridge boost rectifier is one of the most commonly used topologies. In the previously proposed rectifiers, hysteresis control and d-q transformation control were frequently used to control six-switch bridge boosts. Hysteresis control results in variable switching frequency that is difficult for EMI filter design. The d-q approach is based on digital implementation that leads to complicated systems. An encouraging analog solution with constant switching frequency modulation was provided in [5] for a six-switch bridge boost rectifier. However, three-phase voltage is sensed for six-step operation and multipliers are necessary to implement the three phase current references.

In this paper, a general equation that relates input phase voltage and duty ratios of switches is derived for a six-switch bridge boost rectifier based on an average model in Continuous Conduction Mode (CCM). This equation is singular and has infinite solutions. Based on the One-Cycle Control concept [6]-[9] and one solution of this general equation, a Unified Constant-frequency Integration (UCI) Controller is conceived for the standard bridge rectifier that realizes three-phase unity-power-factor and low THD. The proposed controller features the following:

- Constant switching frequency.
- No need for multipliers that are required to scale the current reference according to the load level as used in many other control approaches.
- Three-phase voltage sensor is eliminated.
- Only one integrator with reset along with some logic and linear components are required. It is simple and reliable.

2 The proposed Unified Constant-frequency Integration controller

The analysis in this section is based on following assumption:

- The switches in each arm operate complementary. For example, the duty ratios for switches S_{an}, S_{ap} are d_{an} and $1-d_{an}$ respectively.
- Three-phase system is symmetrical.
- Switching frequency is much higher than line frequency.

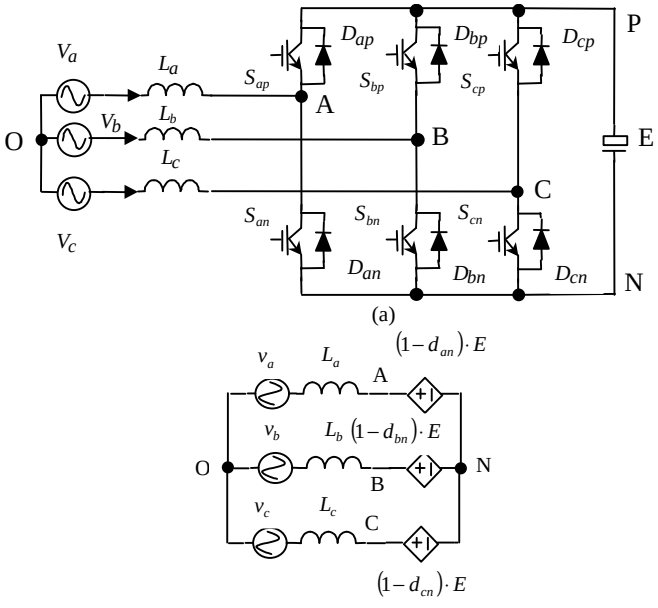

Fig. 1. (a). Three-phase 6-switch bridge boost rectifier. (b) Average model

A six-switch standard bridge boost rectifier is shown in Fig. 1 (a). The average voltages at the node A, B, C referring to node N are given by:

$$\begin{cases} v_{AN} = (1-d_{an})\cdot E \\ v_{BN} = (1-d_{bn})\cdot E \\ v_{CN} = (1-d_{cn})\cdot E \end{cases} \text{----------(1)}$$

where d_{an}, d_{bn}, d_{cn} are the duty ratios for switches S_{an}, S_{bn}, S_{cn}. The equivalent average model for rectifier in Fig. 1 (a) is shown in Fig. 1 (b). The average vector voltage at nodes A, B, C referring to the neutral point "O" equal the phase vector voltages minus the voltage across the inductors L_a, L_b, L_c, as given by

$$\begin{cases} \dot{v}_{AO} = \dot{v}_a - jwL\cdot\dot{i}_{La} \\ \dot{v}_{BO} = \dot{v}_b - jwL\cdot\dot{i}_{Lb} \\ \dot{v}_{CO} = \dot{v}_c - jwL\cdot\dot{i}_{Lc} \end{cases} \text{------(2)}$$

where L is the inductance of input inductors (assuming three-phase inductors are identical), w is the line angular frequency, and $\vec{i}_{La}, \vec{i}_{Lb}, \vec{i}_{Lc}$ are the inductor current vectors. Since these inductors are operating in high frequency and the inductance L is very small regarding to 60Hz utility system, the voltages across the inductors such as $jwL\cdot\vec{i}_{La}$ are very small comparing with the phase voltage and they can be neglected. Therefore, equation (2) can be approximately simplified as

$$\begin{cases} \dot{v}_{AO} \approx \dot{v}_a \\ \dot{v}_{BO} \approx \dot{v}_b \\ \dot{v}_{CO} \approx \dot{v}_c \end{cases} \Rightarrow \begin{cases} v_{AO} \approx v_a = \sqrt{2}\cdot V_i \cdot \sin(wt) \\ v_{BO} \approx v_b = \sqrt{2}\cdot V_i \cdot \sin(wt-120°) \\ v_{CO} \approx v_c = \sqrt{2}\cdot V_i \cdot \sin(wt+120°) \end{cases} \text{-----}$$

-------(3)

For a symmetric three-phase system, it holds that

$$v_a + v_b + v_c = 0 \text{ ------(4)}$$

This leads to

$$v_{AO} + v_{BO} + v_{CO} = 0 \text{---------(5)}$$

The voltages at nodes A, B, C referring to neutral point are given by

$$\begin{cases} v_{AO} = v_{AN} + v_{NO} \\ v_{BO} = v_{BN} + v_{NO} \\ v_{CO} = v_{CN} + v_{NO} \end{cases} \text{---(6)}$$

Combination of equation (5) and (6) yields

$$v_{NO} = -\tfrac{1}{3}\cdot(v_{AN} + v_{BN} + v_{CN}) \text{-------(7)}$$

Substituting equation (7) and (3) into (6) results in

$$\begin{cases} v_{AO} = v_{AN} - \tfrac{1}{3}\cdot(v_{AN} + v_{BN} + v_{CN}) \approx v_a \\ v_{BO} = v_{BN} - \tfrac{1}{3}\cdot(v_{AN} + v_{BN} + v_{CN}) \approx v_b \\ v_{CO} = v_{CN} - \tfrac{1}{3}\cdot(v_{AN} + v_{BN} + v_{CN}) \approx v_c \end{cases} \text{-------(8)}$$

Simplification yields

$$\begin{bmatrix} \frac{2}{3} & -\frac{1}{3} & -\frac{1}{3} \\ -\frac{1}{3} & \frac{2}{3} & -\frac{1}{3} \\ -\frac{1}{3} & -\frac{1}{3} & \frac{2}{3} \end{bmatrix} \cdot \begin{bmatrix} v_{AN} \\ v_{BN} \\ v_{CN} \end{bmatrix} = \begin{bmatrix} v_a \\ v_b \\ v_c \end{bmatrix} \text{-------(9)}$$

Combination of equation (1) and (9) yields the relationship between duty ratio d_{an}, d_{bn}, d_{cn} and voltage v_a, v_b, v_c, which is shown as follows:

$$\begin{bmatrix} -\frac{2}{3} & \frac{1}{3} & \frac{1}{3} \\ \frac{1}{3} & -\frac{2}{3} & \frac{1}{3} \\ \frac{1}{3} & \frac{1}{3} & -\frac{2}{3} \end{bmatrix} \cdot \begin{bmatrix} d_{an} \\ d_{bn} \\ d_{cn} \end{bmatrix} = \frac{1}{E} \cdot \begin{bmatrix} v_a \\ v_b \\ v_c \end{bmatrix} \text{----------(10)}$$

The equation relates average duty ratio of switches to the line voltage. Since the matrix of equation (10) is singular, equation (10) has no unique solution. One possible solution for equation (10) is as follows:

$$\begin{cases} d_{an} = K_1 + K_2 \cdot \dfrac{v_a}{E} \\ d_{bn} = K_1 + K_2 \cdot \dfrac{v_b}{E} \\ d_{cn} = K_1 + K_2 \cdot \dfrac{v_c}{E} \end{cases} \text{--------(11)}$$

Substituting above equation into (10) results in:

Parameter $K_2 = -1$ and K_1 can be any number. Because the duty ratio is less than unity and greater than zero, the following limitation holds

$$0 \le d_{an} = K_1 - \frac{v_a}{E} \le 1 \text{----(12)}$$

The parameter K1 is limited by

$$\frac{v_a}{E} \le K_1 \le 1 + \frac{v_a}{E} \text{--(13)}$$

The equation (11) can be rewritten as

$$\begin{cases} \dfrac{v_a}{E\cdot K_1} = 1 - \dfrac{d_{an}}{K_1} \\ \dfrac{v_b}{E\cdot K_1} = 1 - \dfrac{d_{bn}}{K_1} \\ \dfrac{v_c}{E\cdot K_1} = 1 - \dfrac{d_{cn}}{K_1} \end{cases} \text{--------(14)}$$

For a three-phase rectifier with unity-power-factor, the control goal is given by

$$\begin{cases} v_a = R_e \cdot i_a \\ v_a = R_e \cdot i_a \\ v_a = R_e \cdot i_a \end{cases} \text{-----(15)}$$

where R_e is emulated resistance.

Combination of above equation and (14) yields:

$$\begin{cases} \dfrac{R_e}{E \cdot K_1 \cdot R_S} \cdot R_S \cdot i_a = 1 - \dfrac{d_{an}}{K_1} \\ \dfrac{R_e}{E \cdot K_1 \cdot R_S} \cdot R_S \cdot i_b = 1 - \dfrac{d_{bn}}{K_1} \\ \dfrac{R_e}{E \cdot K_1 \cdot R_S} \cdot R_S \cdot i_c = 1 - \dfrac{d_{cn}}{K_1} \end{cases} \text{----(16)}$$

where parameter R_s is the equivalent current sensing resistor.

Define $V_m = \dfrac{E \cdot R_s \cdot K_1}{R_e}$ ----(17)

where V_m is the output of feedback error compensator.

The equation (16) can be simplified as

$$\begin{cases} R_s \cdot i_a = V_m - V_m \cdot \dfrac{d_{an}}{K_1} \\ R_s \cdot i_b = V_m - V_m \cdot \dfrac{d_{bn}}{K_1} \\ R_s \cdot i_c = V_m - V_m \cdot \dfrac{d_{cn}}{K_1} \end{cases} \text{-------(18)}$$

Three-phase PFC can be achieved by controlling the switches in such a way that the duty ratios and input currents satisfy the equation (18). Replace the currents i_a, i_b, i_c with peak inductor current, the control key equations for peak inductor current sensing are derived as

$$\begin{cases} R_s \cdot i_{Lapk} = V_m - V_m \cdot \dfrac{d_{an}}{K_1} \\ R_s \cdot i_{Lbpk} = V_m - V_m \cdot \dfrac{d_{bn}}{K_1} \\ R_s \cdot i_{Lcpk} = V_m - V_m \cdot \dfrac{d_{cn}}{K_1} \end{cases} \text{----------(19)}$$

The above equation can be implemented with an integrator with reset along with some linear and logic components as shown in Fig. 2 (a). The operation waveforms are shown in Fig. 2 (b); where $Q_{ap}, Q_{an} \cdots Q_{cn}$ are driver signal for switches $S_{ap}, S_{an} \cdots S_{cn}$ respectively. The time constant of the integrator is set to be $t = K_1 \cdot T_S$; where T_S is the switching period. For convenience, K_1 is chosen to be 0.5. In this case, the carrier $V_m - V_m \cdot \dfrac{t}{K_1 \cdot T_S}$ is symmetric to the x axis. The overall schematic for the proposed 3-phase UCI PFC controller with peak inductor current sensing is shown in Fig. 2 (a). No voltage sensors and multipliers are required. In order to prevent short circuit, dead time for complementary switches such as S_{an}, S_{ap} are considered.

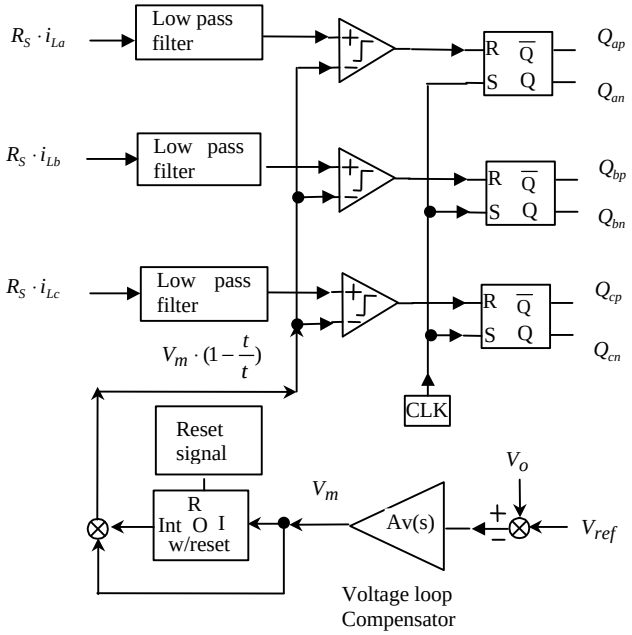

(a)

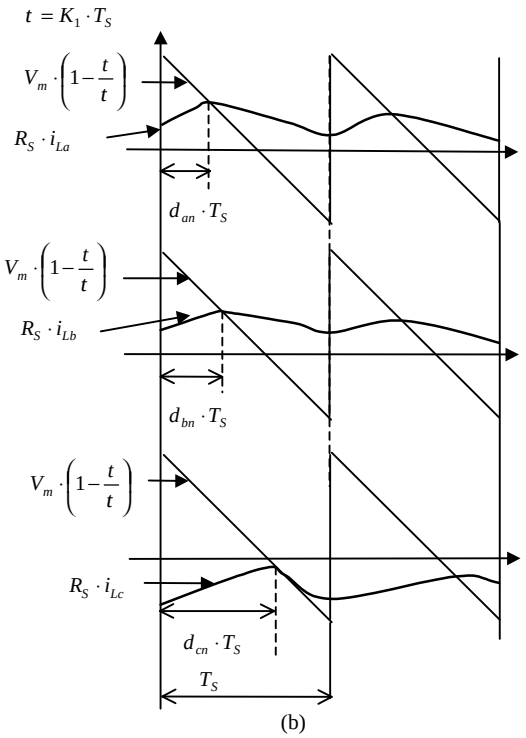

(b)

Fig. 2. (a) Schematic of proposed UCI controller for 3-phae PFC with peak inductor current sensing. (b). Operation waveforms.

For PFC applications, a diode is inserted in the dc bus of the topology in Fig. 1 (a) to prevent the upper and lower switches in one leg from short-through. The reliability is therefore improved. The schematic is shown in Fig. 3.

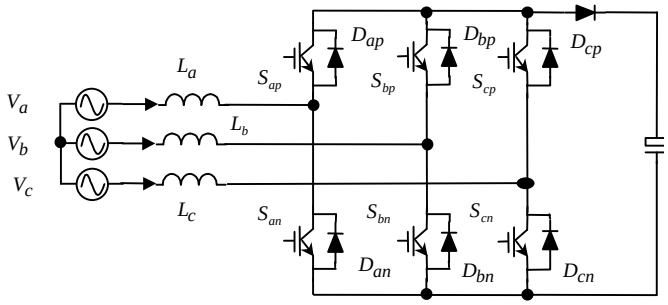

Fig. 3. Three-phase six-switch boost rectifier with a dc diode.

3 Limitation of the proposed control approach

With the proposed approach, the inductor current will experience larger distortion at light load. It is found that in certain region of the line cycle, the inductor current could be "partly uncontrolled". This phenomena occurs when V_m is small and load is light. The open loop simulation under this condition is shown in Fig. 4, where $V_m \cdot \left(1-\frac{t}{0.5 \cdot T_s}\right)$ is the carrier, $R_s \cdot i_{La}$, $R_s \cdot i_{Lb}$, $R_s \cdot i_{Lc}$ are the sensed inductor currents, and Q_{an} Q_{bn} Q_{cn} are driving signals for switches S_{an}, S_{bn}, S_{cn} respectively. Simulation conditions are as follows: the input inductance is 1mH; the switching frequency is 10kHz; the current sensing resistance is 0.2ohm; the output voltage is 500V, and the voltage $V_m = 1V$. Fig. 4 (a) shows the switching cycle operation waveforms and Fig. 4 (b) shows the line-cycle inductor current. In this case, the sensed signal $R_s \cdot i_{La}$ is above the envelope of carrier signal $V_m \cdot \left(1-\frac{t}{0.5 \cdot T_s}\right)$, which indicates uncontrolled operation in a small region.

The reason for this uncontrolled operation is due to the redundancy of switching states during each switching cycle. In the beginning of each switching cycle, all the lower switches S_{an}, S_{bn}, S_{cn} are turned on and the equivalent circuit is shown in Fig. 5 (a). Near end of the switching cycle when all of these three switches are turned off, all the upper leg switches S_{ap}, S_{bp}, S_{cp} are turned on. The equivalent circuit is shown in Fig. 5 (b). The electrical property for these two states is identical to each other. For both cases, the inductor voltage equals phase voltage and inductor currents increase. Take phase B as an example as shown in Fig. 4 (a). When Q_{bn} is off, the inductor current i_{Lb} increases with a slope of $\frac{v_b(t)}{L}$ (At this time, phase v_b is negative).

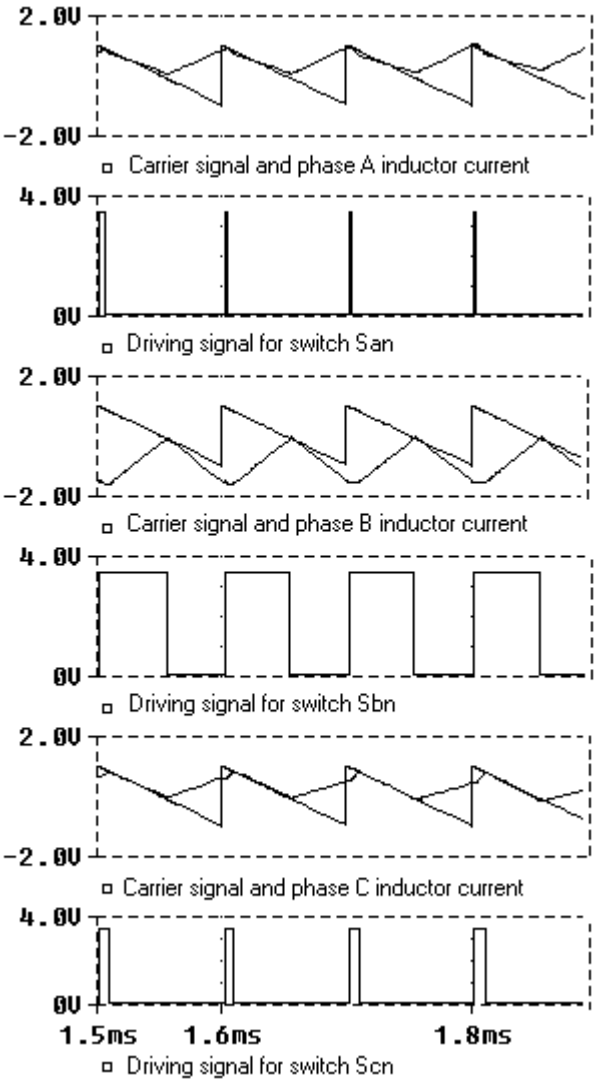

(a)

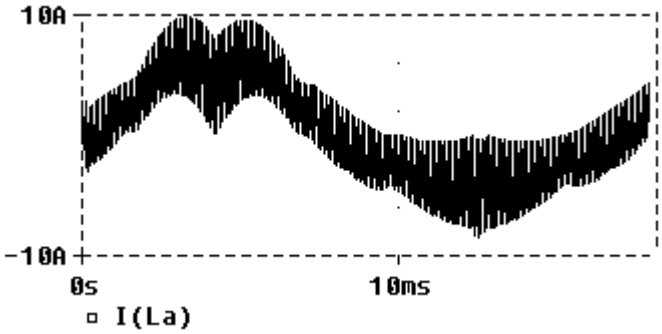

(b)

Fig. 4. Simulated waveforms when inductor current is "partly uncontrolled" at light load .

If the slope of inductor current is greater than the equivalent slope of ramp signal $V_m \cdot \left(1-\frac{t}{0.5 \cdot T_s}\right)$, the current will grow beyond the envelope. To avoid this situation, a circuit limitation is required, that is

$$R_s \cdot \frac{v_b(t)}{L} \le \frac{V_m}{t}.$$

The inductor should be chosen according to equation (20)

$$L \ge R_s \cdot \frac{V_{g\max}}{\min(V_m)} \cdot t \quad \text{-------(20)}$$

where R_s is the current sensing resistance; $V_{g\max}$ is the peak of the input phase voltage; t is the integration time constant ($t = 0.5T_s$ is chosen in this paper); $\min(V_m)$ is the minimum voltage of V_m that determines the minimum load by equation (17).

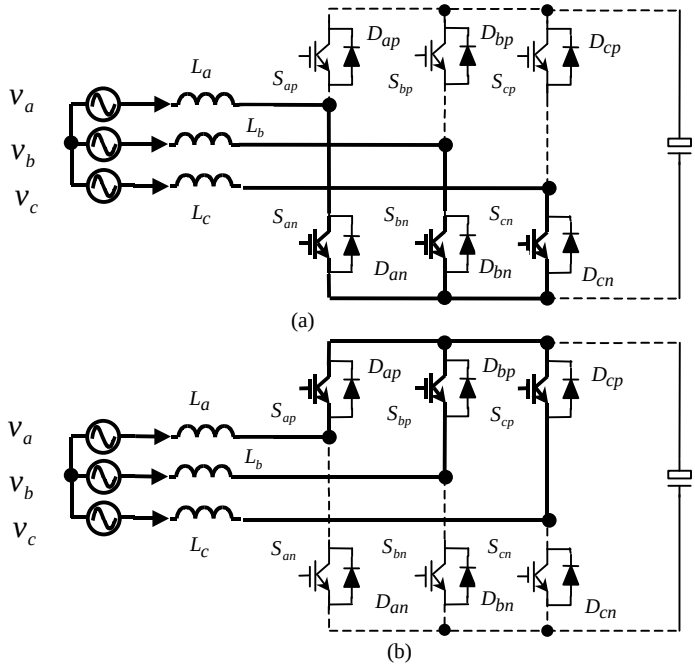

Fig. 5. Equivalent circuit when three lower leg switches are turned on (a) or three upper leg switches are turned on (b).

4 Experimental verification

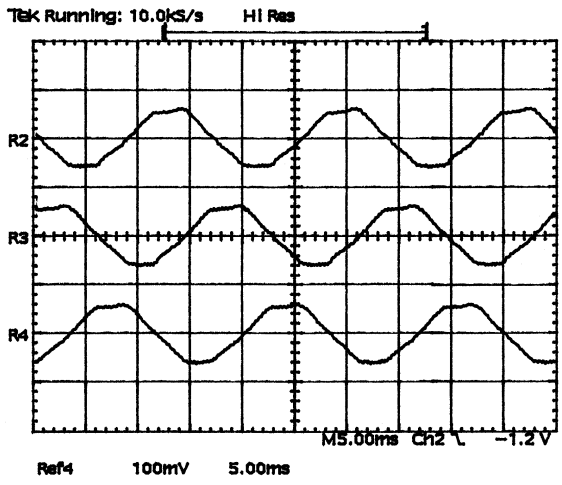

Fig. 6. Three-phase inductor current waveforms. R2: i_{La}, 5A/div. R3: i_{Lb}, 5A/div. R4: i_{Lc}, 5A/div

In order to verify the concept, an experimental circuit was built that employs the three-phase boost rectifier with dc diode in Fig. 3. The experimental waveforms are shown in Fig. 6. The parameters are as follows: main inductance is 300uH; the switching frequency is 50kHz. The input voltage is 90Vrms. The output voltage is 420V. The output resistance is 327ohm and output power is 540watts. The measured input current THD is 7.5% while the input voltage has about 4% THD itself.

5 Conclusion

In this paper, a three-phase six-switch boost rectifier is investigated. The relationship between input phase voltage and switch duty ratios is given by a singular equation. Based on one of solutions and using One-Cycle Control, a UCI controller is proposed to achieve three-phase unity-power-factor. The proposed controller employs constant frequency modulation that is desirable for industrial applications. It is composed of one integrator with reset along with some linear and logic components. No multipliers and input voltage sensors are used. Nearly unity power factor was demonstrated experimentally in all three phases using this simple control circuit. The input current distortion is higher for light load operation. Design criteria are given to improve the current distortion at light load.

References

[1] P.D Ziogas, "An Active Power Factor Correction Technique for Three-Phase Diode Rectifiers", IEEE Trans on power electronics, vol,6, No 1. Jan, 1991.

[2] Kolar, J.W; Zach, F.C. "A novel three-phase utility interface minimizing line current harmonics of high power telecommuncations rectifiers modules", IEEE Trans on Industrial Electronics, vol. 44, IEEE, Aug. 1997. P.456-67.

[3] J.C. Salmon, " Comparative evaluation of circuit topologies for 1-phase and 3-phase boost rectifiers operated with a low current distortion", Proceeding of Canadian Conference on Electrical and Computer Engineering, 1994. p.30-3. Vol. 1

[4] J. C. Salmon, E. Nowicki: "Operation, control and performance of a family of high power unity power factor rectifiers", Proceeding of Canadian Conference on Electrical and Computer Engineering, 1995, p.854-7.

[5] Mao, H, Boroyevich, D. and Lee, F.C: "Analysis and design of high frequency three-phase boost rectifiers", APEC '96, p538-44.

[6] Smedley, K. and Cuk, S. "One-cycle control of switching converter", PESC, 1991.

[7] Lai, Z, and Smedley,K.M. "A General Constant Frequency Pulse-Width Modulator and Its Applications". IEEE Transactions on Circuits and Systems I: Fundamental Theory and Applications, vol 45.(no.4), IEEE, April, 1998.P.386-96.

[8] Qiao, C. and Smedley, K.M. "A General Three-Phase PFC Controller. Part I for rectifiers with a Parallel-connected Dual Boost Topology", IEEE IAS'99.

[9] Qiao, C. and Smedley, K.M. "A General Three-Phase PFC Controller. Part II for rectifiers with a Series-connected Dual Boost Topology", IEEE IAS'99.